Study of $\psi' \to \pi^+\pi^- J/\psi$

F. A. Harris
Department of Physics and Astronomy
The University of Hawaii
2505 Correa Road
Honolulu, HI 96822
USA

July 6, 1998

Introduction

The process $\psi' \to \pi^+\pi^- J/\psi$ can be investigated using the very clean, high statistics $\psi' \to \pi^+\pi^- J/\psi$, $J/\psi \to l^+l^-$ events. For this case, the dipion invariant mass distribution is very different from that expected from phase space [1], and a number of authors have proposed various theoretical models [2]-[6]. The reaction is pictured as the radiation of two gluons by the quarkonium system as it transfers to the lower energy level, followed by the hadronization of the gluons into pions.

There is increased interest in this process because of the problems with the $\Upsilon(3S) \to \pi^+\pi^-\Upsilon(1S)$ [7], which has a peak at low mass, as well as a peak at high mass. This distribution looks very different than $\psi' \to \pi^+\pi^- J/\psi$, which has a high mass peak, and most theoretical models. The process $\Upsilon(2S) \to \pi^+\pi^-\Upsilon(1S)$ is similar to $\psi' \to \pi^+\pi^- J/\psi$ but not the same.

In this paper, we will use the $\psi' \to \pi^+\pi^- J/\psi$ process to test models. This is the third in a series of informal analysis notes, and much of the background necessary for this paper is described in more detail in the first two notes [8] [9]. The work on this subject is continuing and the results shown in this paper are quite preliminary.

Cuts

Pion Cuts:

The initial pion cuts are the same as in Ref. [8] but are given again for convenience.

- good run (PPRUNS: status > 1)
- mnfit = 2, -9, -19
- $|\cos\theta| < 0.75$ for π's

- $p_\pi < 0.5$ GeV/c
- $pxy(\pi) > 0.1$ GeV/c
- $\cos\theta_{\pi\pi} < 0.9$ $\theta_{\pi\pi}$ is the laboratory angle between the π^+ and π^-. This cut is used to eliminate contamination from misidentified e^+e^- pairs from γ conversions.
- $3.0 < m_{recoil} < 3.2$ GeV/c^2

These are the cuts used to select events for determining $B(J/\psi \rightarrow l^+l^-)$, where a fit is done to determine the number of $\psi' \rightarrow \pi^+\pi^- J/\psi$, $J/\psi \rightarrow l^+l^-$ events. However when selecting a sample for other purposes, like studying $\psi' \rightarrow \pi^+\pi^- J/\psi$, additional cuts are made on the π's to reduce background. The additional cuts are:

- $\Sigma Hit_\pi^{dE/dx} > 13$. $\Sigma Hit_\pi^{dE/dx}$ is the number of hits used in the dE/dx calculation.
- $|\chi_\pi^{dE/dx}| < 3.0$. $\chi_\pi^{dE/dx} = \frac{(dE/dx)_{meas} - (dE/dx)_{exp}}{\sigma}$.

Lepton Cuts

- Events must satisfy PID requirements described in Ref. [9].
- $0.5 < p_l < 2.5$ GeV/c
- $|\cos\theta| < 0.75$ for electrons, < 0.60 for muons.
- $\cos\theta_{l^+l^-} < -0.85$. This is the cosine of the angle between the two leptons in the lab. The leptons from this decay are almost back to back.
- $\cos\theta_{l^+l^-}^{cm} < -0.975$. This is the cosine of the angle between the two leptons in the J/ψ CM. The leptons are even more back-to-back in the CM system.
- p_{l^+} or $p_{l^-} > 1.3$ GeV/c or $p_{l^+} + p_{l^-} > 2.4$ GeV/c. This cut is used to remove background.

Additional Cuts

We make additional cuts in order to reduce background from events where the low energy pions undergo $\pi \rightarrow \mu\nu$ decay or where the leptons (especially electrons) radiate much of their energy. These cuts are necessary for comparisons with theoretical models.

- good tracks: mfit = 2
- vertex cuts:
  - $|rm(\pi)| < 0.015m$
  - $|zm(\pi)| < 0.15m$
  - $|zm(\pi^+) - zm(\pi^-)| < 0.05m$
- $3.07 < m_{recoil} < 3.12$ GeV/c^2
- $|m_{l^+l^-} - m_{J/\psi}| < 0.25$ GeV/c^2

A total of about 22.8 K events remains after these cuts.

Monte Carlo

The Monte Carlo generator used is PPGEN. A total of 200,000 (153 realization) plus 370,000 (154 realization) Monte Carlo events are generated each for the $\psi' \to \pi^+\pi^- J/\psi$, $J/\psi \to e^+e^-$ and $\psi' \to \pi^+\pi^- J/\psi$, $J/\psi \to \mu^+\mu^-$ samples. The Monte Carlo[10] assumes:

1. The orbital angular momentum between $\pi\pi$ system and J/ψ and between π's in the $\pi^+\pi^-$ system is 0.

2. The mass of the $\pi\pi$ system is weighted towards high mass.

$$\frac{d\sigma}{dm_{\pi\pi}} \propto (\text{phase space}) \times (m_{\pi\pi}^2 - 4m_\pi^2)^2$$

3. Sequential 2-body decays: $\psi' \to X + J/\psi$, $X \to \pi^+\pi^-$, and $J/\psi \to l^+l^-$.

4. X and J/ψ are uniformly distributed in $\cos\theta$.

5. π's are uniformly distributed in $\cos\theta_\pi$ in the X rest frame.

6. Leptons have $1 + \cos^2\theta$ distribution in J/ψ rest frame.

7. J/ψ decay has order α^3 final state radiative correction in rest frame of the J/ψ.

Comparison with Monte Carlo Distributions

In Ref. [9], comparisons were made between data and Monte Carlo data for various distributions. In general the agreement was good, indicating that the cuts eliminated most background and that the Monte Carlo did a reasonable job of representing the data. However some distributions, like the $m_{\mu^+\mu^-}$ distribution, did not agree well, possibly indicating an inadequacy in the realization.

Here we compare other distributions to check whether the assumptions made by the Monte Carlo are correct. In order to be able to compare to theoretical models, we correct the distributions for detection efficiency. Monte Carlo data is run through the same analysis program as the data. A bin by bin efficiency is then determined for each distribution of interest using the generated and detected Monte Carlo data. This bin by bin efficiency is then used to correct each bin of the data distributions.

In Fig. 1, we see reasonable agreement between data and Monte Carlo except in Fig. 1d, which is the distribution of the cosine of the angle between the π^+ and the J/ψ direction in the rest frame of the $\pi\pi$ system, $\cos\theta_{\pi^+}$. The flat Monte Carlo distribution is due to the assumption that the relative angular momentum of the 2 π's is S-wave. The disagreement between data and Monte Carlo data casts doubt on this assumption.

Fig. 1a indicates that the $m_{\pi\pi}$ distribution agrees fairly well but not perfectly with the assumed empirical distribution. Fig. 1b indicates agreement with the assumed $1+\cos^2\theta_l$ distribution for the leptons in $\psi' \to \pi^+\pi^- J/\psi$, $J/\psi \to l^+l^-$ events. The flat distribution in Fig. 1c is related to the assumption that the relative angular momentum between the $\pi\pi$ system and the J/ψ is zero.

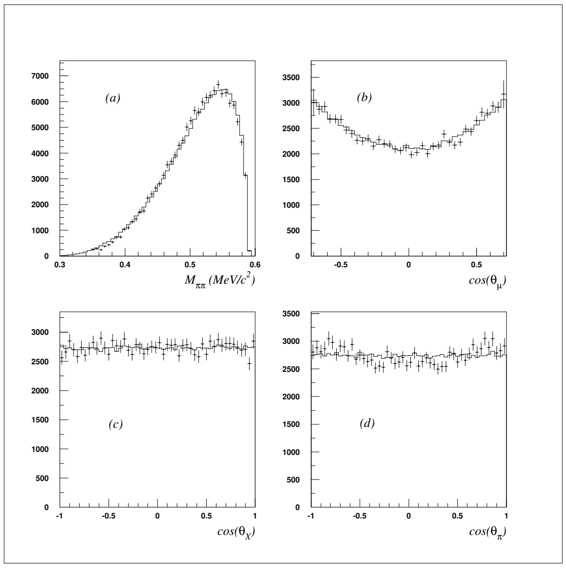

Figure 1: Various distributions (corrected for detection efficiency) for $\psi' \to \pi^+\pi^- J/\psi$, $J/\psi \to l^+l^-$ decays. **a.)** $m_{\pi^+\pi^-}$ distribution. The distribution is in fair but not perfect agreement with the assumed empirical distribution. **b.)** $\cos\theta_l$ distribution. The assumed distribution is a $1+\cos^2\theta_l$ distribution. This angle is the angle between the beam direction and the e^+ in the rest frame of the J/ψ. **c.)** $\cos\theta_X$ distribution. This is the cosine of the angle of the $\pi\pi$ system with respect to the e^+e^- direction in the e^+e^- CM system. The distribution for Monte Carlo data is flat because of the S-wave assumption for the relative angular momentum of the $\pi\pi$ system and the J/ψ. **d.)** $\cos\theta_{\pi^+}$ distribution. This is the cosine of the angle of the π^+ with respect to the J/ψ direction in the $\pi\pi$ rest frame. The Monte Carlo distribution is flat because of the assumption that the relative angular momentum of the π's is S-wave. The data agree well with the Monte Carlo except in d.).

Fig. 2 shows the ϕ angle distributions for the l^+ in the J/ψ rest frame, J/ψ in the lab, and the π^+ in the rest frame of the $\pi\pi$ system. All distributions are uniform in ϕ, consistent with the Monte Carlo assumptions.

Since Fig. 1d indicates an inadequacy with the Monte Carlo, it is necessary to correct our bin-by-bin efficiency determination in our following studies. We will use the Novikov-Shifman model (discussed later) to determine a weighting for Monte Carlo events so that the proper efficiency is determined as a function of $\cos\theta_\pi$ and $m_{\pi\pi}$.

Angular Distributions in $\psi' \to \pi^+\pi^- J/\psi$

In this section, we will compare our angular distributions with the general decay amplitude analysis of Cahn [11]. The ψ' and ψ have $J^P = 1^-$ and $I^{GC} = 0^{--}$, while the $\pi\pi$ system has $I^{GC} = 0^{++}$. At an e^+e^- machine, the ψ' is produced with polarization transverse to the beam. The decay of ψ' is treated as a 2-body decay:

$$\psi' \to XJ/\psi, X \to \pi^+\pi^-,$$

which can be described by the quantum numbers:

$\vec{l}$ – $\pi\pi$ angular momentum

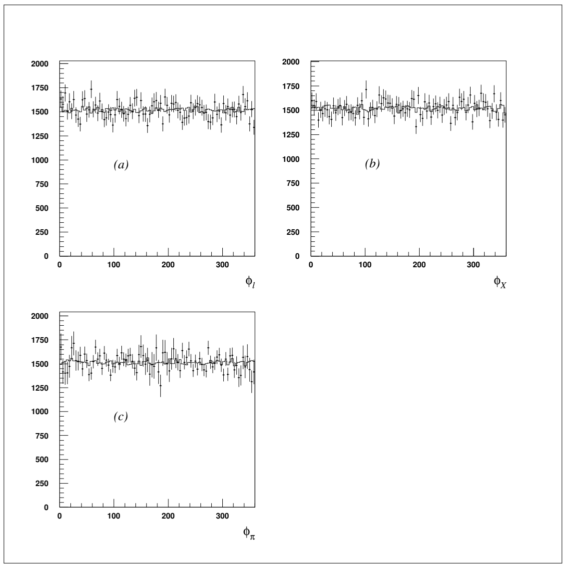

Figure 2: Azimuthal angle distributions (corrected for detection efficiency) for $\psi' \to \pi^+\pi^- J/\psi$, $J/\psi \to l^+l^-$ decays. a.) The ϕ angle distribution for the l^+ in the J/ψ rest frame. b.) The ϕ angle distribution for the J/ψ in the lab. c.) The ϕ angle distribution for the π^+ in the rest frame of the $\pi\pi$ system.

$\vec{\boldsymbol{L}}$ $-$ ψ X angular momentum

$\vec{\boldsymbol{s}}$ $-$ spin of ψ

$\vec{\boldsymbol{s}}\,'$ $-$ spin of the ψ'

Defining $\vec{S} = \vec{s} + \vec{l}$, called the channel spin, then $\vec{s}\,' = \vec{S} + \vec{L} = \vec{s} + \vec{l} + \vec{L}$. An eigenstate of $J^2 = s'^2$, L^2, S^2, and J_z may be constructed. Parity conservation and charge conjugation invariance require both L and l to be even.

The decay can be described in terms of partial waves. Cahn works out the angular distributions in terms of partial wave amplitudes, $M_{l,L,S}$. The partial waves can be truncated after a few terms. He says, "For the purpose of demonstration, and with simplicity as a criterion, consider only M_{001}, M_{201}, and M_{021}". Cahn's 1-dimensional distributions:

$$\frac{d\Gamma}{d\Omega_\psi} \propto [|M_{001}|^2 + |M_{201}|^2 + \frac{1}{4}|M_{021}|^2(5 - 3\cos^2\theta_\psi)] \tag{1}$$

$$\frac{d\Gamma}{d\Omega_\pi} \propto [|M_{001}|^2 + \frac{1}{4}|M_{201}|^2(5 - 3\cos^2\theta_\pi) + |M_{021}|^2] \tag{2}$$

$$\frac{d\Gamma}{d\Omega_\mu} \propto [|M_{001}|^2(1 + \cos^2\theta_\mu) + \frac{1}{10}(|M_{201}|^2 + |M_{021}|^2)(13 + \cos^2\theta_\mu)] \tag{3}$$

The $d\Omega$'s are measured in their respective rest frames. It is understood that the $M_{l,L,S}$ are functions of $m_{\pi\pi}$.

It turns out that Eqns. 1 and 2 are incorrect! This is suggested by Fig. 1d. We see that the data indicates that the distribution is concave upwards, while Eqn. 2 would suggest that the distribution must be concave downwards if M_{201} is nonzero. It is nice to have data to check theory!

To find the correct 1D distributions, we start with Cahn's full expression [11], which we assume is correct. We then integrate over $d\Omega_\mu$ using Mathematica and find:

$$\begin{aligned}\frac{d\Gamma}{d\Omega_\pi d\Omega_\psi} \propto\ & |M_{001}|^2 + |M_{201}|^2(\frac{5}{4} - \frac{3}{4}\cos^2\theta_\pi) + |M_{021}|^2(\frac{5}{4} - \frac{3}{4}\cos^2\theta_\psi) \\ & +2\Re\{M_{201}M_{001}^*\}[\frac{1}{\sqrt{2}}(\frac{3}{2}\cos^2\theta_\pi - \frac{1}{2})] \\ & +2\Re\{M_{021}M_{001}^*\}[\frac{1}{\sqrt{2}}(\frac{3}{2}\cos^2\theta_\psi - \frac{1}{2})] \\ & +2\Re\{M_{201}M_{021}^*\}[\frac{9}{8}\sin^2\theta_\pi\sin^2\theta_\psi\cos 2(\phi_\pi - \phi_\psi) \\ & +\frac{9}{16}\sin 2\theta_\pi \sin 2\theta_\psi \cos(\phi_\pi - \phi_\psi) \\ & +\frac{1}{2}(\frac{3}{2}\cos^2\theta_\pi - \frac{1}{2})(\frac{3}{2}\cos^2\theta_\psi - \frac{1}{2})]\end{aligned} \tag{4}$$

This agrees with Cahn except for obvious typos. We can then integrate to find the corrected 1-D distributions:

$$\frac{d\Gamma}{d\Omega_\psi} \propto [|M_{001}|^2 + |M_{201}|^2 + \frac{1}{4}|M_{021}|^2(5 - 3\cos^2\theta_\psi) + \frac{1}{\sqrt{2}}\Re\{M_{021}M_{001}^*\}(3\cos^2\theta_\psi - 1)] \tag{5}$$

$$\frac{d\Gamma}{d\Omega_\pi} \propto [|M_{001}|^2 + \frac{1}{4}|M_{201}|^2(5 - 3\cos^2\theta_\pi) + |M_{021}|^2 + \frac{1}{\sqrt{2}}\Re\{M_{201}M_{001}^*\}(3\cos^2\theta_\pi - 1)] \tag{6}$$

Two of Cahn's 1D distributions (Eqns. 1 and 2) dropped the interference term. It is the interference term in Eqn. 6 that allows the equation to be consistent with the data. Eqn. 3 is correct.

Fits to 1D Angular Distributions

There are too many unknowns to fit the 1D distributions separately, but we can fit them simultaneously. There are 3 complex numbers to be obtained. According to Cahn, if the ψ' and ψ are regarded as inert, then the usual final state argument gives $M_{l,L,S} = e^{i\delta_l^0(m_{\pi\pi})}|M_{l,L,S}|$, where $\delta_l^0(m_{\pi\pi})$ is the isoscalar phase shift for quantum number l. If we interpolate the S wave, isoscalar phase shift data found in [12], we find $\delta_0^0 \approx 45^o$. However it does change with $m_{\pi\pi}$. Also δ_2^0 is supposed to be ≈ 0. Using these values as input, we obtain the combined fit shown in Fig. 3 and the results given in Table 1. The fitting procedure also uses two parameters (not shown), which correspond to the relative normalizations of the second and third distributions relative to the first. Also given in Table 1 are the ratios M_{201}/M_{001} and M_{021}/M_{001}.

We have also tried to obtain $\delta_0^0(m_{\pi\pi})$, as well as the three real amplitudes. Cahn points out that one of the advantages of the process $\psi' \to \pi^+\pi^- J/\psi$ is that it allows us to obtain δ_0^0, which is not measured in this mass range. The results from the fit are given in Table 2. Minuit indicates that there are problems with the fit. Both fits yield a nonzero result for M_{201}, indicating non negligible D-wave in the $\pi\pi$ system. The amplitude M_{021} is very small, indicating the the ψX angular momentum is consistent with zero.

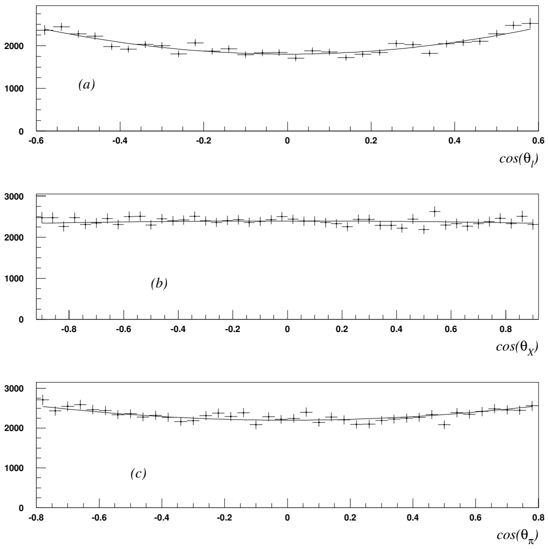

Figure 3: Simultaneous fits (χ^2) to three 1-D histograms of (a) $\cos\theta_\mu$, (b) $\cos\theta_X$, and (c) $\cos\theta_\pi$ using Eqns. 3, 5, and 6, respectively. The phase shifts used are $\delta_0^0 = 45^o$ and $\delta_2^0 = 0^o$.

Fits to the 2D Distribution

We can integrate Eqn. 4 over the ϕ angles to obtain an expression that depends only on $\cos\theta_\pi$ and $\cos\theta_\psi$:

$$\begin{aligned}\frac{d\Gamma}{d\cos\theta_\pi d\cos\theta_\psi} \propto\ & |M_{001}|^2 + |M_{201}|^2(\frac{5}{4} - \frac{3}{4}\cos^2\theta_\pi) + |M_{021}|^2(\frac{5}{4} - \frac{3}{4}\cos^2\theta_\psi) \\ & +2\Re\{M_{201}M_{001}^*\}[\frac{1}{\sqrt{2}}(\frac{3}{2}\cos^2\theta_\pi - \frac{1}{2})] \\ & +2\Re\{M_{021}M_{001}^*\}[\frac{1}{\sqrt{2}}(\frac{3}{2}\cos^2\theta_\psi - \frac{1}{2})]\end{aligned}$$

Table 1: Results of simultaneous χ^2 fits to the three 1-D distributions of $\cos\theta_\mu$, $\cos\theta_X$, and $\cos\theta_\pi$ shown in Fig. 3. The phase shifts used are $\delta_0^0 = 45^o$ and $\delta_2^0 = 0^o$. The amplitude normalizations are arbitrary. Two other fit parameters (not shown) are the normalizations of the second and third distributions relative to the first.

M_{001}	41.6 ± 0.36
M_{201}	7.5 ± 1.4
M_{021}	-0.56 ± 0.60
M_{201}/M_{001}	0.18 ± 0.03
M_{021}/M_{001}	-0.014 ± 0.014
χ^2/DF	0.8

Table 2: Results of simultaneous χ^2 fits to the three 1-D distributions of $\cos\theta_\mu$, $\cos\theta_X$, and $\cos\theta_\pi$ using Eqns. 3, 5, and 6. Here the phase shift δ_0^0 is determined from the fit. δ_2^0 is taken to be 0^o. The amplitude normalizations are arbitrary. Two other fit parameters (not shown) are the normalizations of the second and third distributions relative to the first.

M_{001}	42.0 ± 0.4
M_{201}	5.0 ± 2.5
M_{021}	-0.55 ± 0.61
δ_0^0	0 ± 56^o
M_{201}/M_{001}	0.12 ± 0.06
M_{021}/M_{001}	-0.013 ± 0.014
χ^2/DF	0.8
Fit result:	problems

$$+\Re\{M_{201}M_{021}^*\}[(\frac{3}{2}\cos^2\theta_\pi - \frac{1}{2})(\frac{3}{2}\cos^2\theta_\psi - \frac{1}{2})] \tag{7}$$

We can then fit the 2D distribution of $\cos\theta_\pi$ versus $\cos\theta_\psi$ using this equation. We first fit assuming $\delta_0^0 = 45^o$ and $\delta_2^0 = 0^0$, as was done previously. Using these values, we obtain the fit values shown in Table 3. The 1D projections of the 2D distribution along with the fit projections are shown in Fig. 4.

We have also performed the fits for different $m_{\pi\pi}$ intervals for $\delta_0^0 = 45^o$ and $\delta_2^0 = 0^0$. The results are shown in Table 4. The ratios M_{201}/M_{001} and M_{021}/M_{001} do not show large variation between the three interval, and M_{201}/M_{001} is inconsistent with zero for all intervals.

Table 3: Result of the 2-D Likelihood fit to $\cos\theta_\pi$ versus $\cos\theta_X$ using Eqn. 7. The phase shifts used are $\delta_0^0 = 45^o$ and $\delta_2^0 = 0^o$. The amplitude normalizations are arbitrary.

M_{001}	13.6 ± 0.08
M_{201}	2.3 ± 0.5
M_{021}	0.05 ± 0.22
M_{201}/M_{001}	0.17 ± 0.04
M_{021}/M_{001}	0.004 ± 0.02
χ^2/DF	1.1

We can also assume that δ_2^0 is zero and fit for δ_0^0. The results of this fits is shown in Table 5. Note that PAW says that this fit has problems, so the results are not meaningful.

In comparing the results from Tables 1-5, we see that M_{201}/M_{001} varies between 0.12 and 0.18 and is at least two sigma from zero. On the other hand M_{021}/M_{001} varies between 0 and 0.06 and is, in almost all cases, consistent with zero. Only for the lowest $m_{\pi\pi}$ region is it more than one standard deviation from zero. When we try to fit for δ_0^0, the fits have problems in Minuit. We are unable to determine the phase angle.

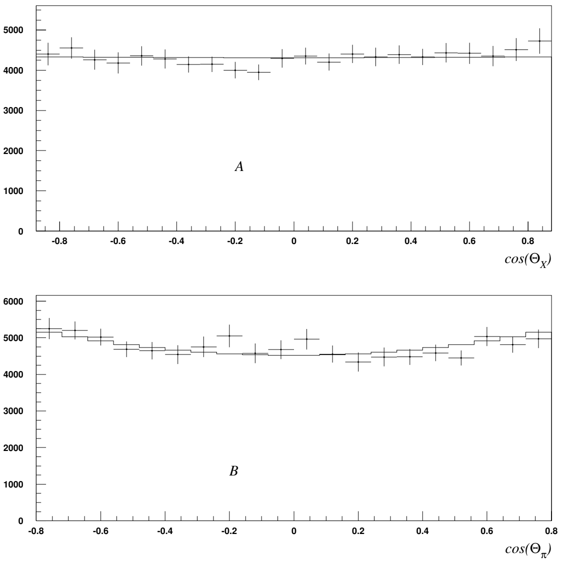

Figure 4: Likelihood fit result for $\cos\theta_X$ versus $\cos\theta_\pi$ using Eqn. 7. The phase shifts used are $\delta_0^0 = 45^o$ and $\delta_2^0 = 0^o$. a.) The projection of $\cos\theta_X$ and the fit result. b.) The projection of $\cos\theta_\pi$ and the fit result. Points with error bars are the data; the histogram is the fit result.

Model Independent Fit of the $\cos\boldsymbol{\theta}_\pi$ as a Function of $\boldsymbol{m}_{\pi\pi}$

The amount of D wave as a function of $m_{\pi\pi}$ has been fit using

$$N(\cos\theta) \propto 1.0 + p * (\cos^2\theta - 1/3) + q * (\cos^2\theta - 1/3)^2 \tag{8}$$

The last term corresponds to the amount of D-wave, while the middle term corresponds to the interference term. The results are shown in Fig. 5 and in Table 6. It can be seen that q is consistent with zero. The behavior of the interference term, p, as a function of $m_{\pi\pi}$ is shown in Fig. 6.

Table 4: Results of the 2-D Likelihood fits to $\cos\theta_\pi$ versus $\cos\theta_X$ using Eqn. 7 for different $m_{\pi\pi}$ intervals. The amplitude normalization is arbitrary.

$m_{\pi\pi}$ Range (GeV/c^2)	0.36 - 0.5	0.5 - 0.54	0.54 - 0.6
M_{001}	8.36 ± 0.06	7.43 ± 0.06	7.86 ± 0.13
M_{201}	1.19 ± 0.37	0.89 ± 0.41	1.37 ± 0.50
M_{021}	0.53 ± 0.27	-0.27 ± 0.21	0.14 ± 0.20
M_{201}/M_{001}	0.14 ± 0.04	0.12 ± 0.06	0.17 ± 0.06
M_{021}/M_{001}	0.06 ± 0.03	-0.04 ± 0.03	0.02 ± 0.03
χ^2/DF	1.3	1.5	1.3
Events	6186	7075	9362

Table 5: Result of the 2-D Likelihood fit to cos θ_π versus cos θ_X using Eqn. 7. Here the phase shift δ_0^0 is determined from the fit. The amplitude normalization is arbitrary.

M_{001}	13.68 ± 0.14
M_{201}	1.85 ± 0.7
M_{021}	0.05 ± 0.22
M_{201}/M_{001}	0.14 ± 0.05
M_{021}/M_{001}	0.0 ± 0.02
δ_0^0	32 ± 33^o
χ^2/DF	1.1
Fit result	problems

Table 6: Fit results to cos θ_π distribution using a χ^2 fit to Eqn. 8. The fit also requires a normalization term which is not shown.

$m_{\pi\pi}$ Range (GeV/c^2)	p	q	χ^2/DOF	Events/ϵ
0.34 - 0.42	0.67 ± 0.67	-0.1 ± 2.4	0.7	6130
0.42 - 0.45	0.41 ± 0.38	-0.6 ± 1.5	0.8	7700
0.45 - 0.48	0.15 ± 0.16	-0.16 ± 0.74	0.8	12700
0.48 - 0.51	0.30 ± 0.10	0.18 ± 0.51	0.8	21200
0.51 - 0.54	0.08 ± 0.06	-0.04 ± 0.19	0.7	27500
0.54 - 0.57	0.15 ± 0.05	-0.13 ± 0.17	1.0	28100
0.57 - 0.60	0.08 ± 0.09	0.07 ± 0.28	1.0	11900

Comparison with Heavy Quarkonium Models

Novikov-Shifman Model

The first comparison of BES data with Heavy Quark models was presented at BES95 by Fan Jingyun [13]. The model investigated was the Novikov-Shifman [3] model, which has the amplitude:

$$\begin{aligned} A &\propto \{q^2 - \kappa(\Delta M)^2(1 + \frac{2m_\pi^2}{q^2}) \\ &\quad + \frac{3}{2}\kappa[(\Delta M)^2 - q^2](1 - \frac{4m_\pi^2}{q^2})(\cos^2\theta_\pi - \frac{1}{3})\}, \end{aligned} \tag{9}$$

where q is the 4 momentum of the dipion system and $\Delta M = M_{\psi'} - M_{J/\psi}$. The parameter κ is given by:

$$\kappa = (b/6\pi)\alpha_s(\mu)\rho_\mu^G(\mu), \tag{10}$$

where $b = 9$ is the first expansion coefficient of the Gell-Mann-Low function, ρ^G is the gluon share of the π's momentum, which is about 0.4, and κ is predicted to be ≈ 0.15 to 0.2 [4]. From Eqn. 10,

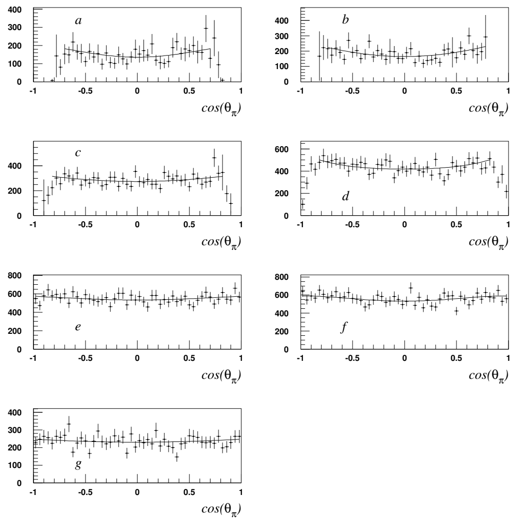

Figure 5: Fits of $\cos\theta_\pi$ using Eqn. 8 as a function of $m_{\pi\pi}$. The fit results are shown in Table 6. **a)** $0.34 < m_{\pi\pi} < 0.42$ GeV/c^2, **b)** $0.42 < m_{\pi\pi} < 0.45$ GeV/c^2, **c)** $0.45 < m_{\pi\pi} < 0.48$ GeV/c^2, **d)** $0.48 < m_{\pi\pi} < 0.51$ GeV/c^2, **e)** $0.51 < m_{\pi\pi} < 0.54$ GeV/c^2, **f)** $0.54 < m_{\pi\pi} < 0.57$ GeV/c^2, and **g)** $0.57 < m_{\pi\pi} < 0.60$ GeV/c^2,

it can be seen that κ is expected to be different for $\psi(2S)$ decays and the decays of other charmonia, because of the running of α_s. The first terms in the amplitude are the S-wave contribution, and the last term is the D-wave contribution. Note that parity and charge conjugation invariance require that the spin be even. If κ is non-zero, it is predicted that there should be some D-wave. However, since κ is expected to be small, the process should be predominantly S-wave.

The differential cross section is obtained by squaring the amplitude and multiplying by phase space.

$$\frac{d\Gamma}{dm_{\pi\pi}d\cos\theta} \propto (\mathrm{PS}) \times A^2. \tag{11}$$

where

$$PS = \sqrt{\frac{(m_{\pi\pi}^2 - 4m_\pi^2)[M_{J/\psi}^4 + M_{\psi'}^4 + m_{\pi\pi}^4 - 2(M_{J/\psi}^2 m_{\pi\pi}^2 + M_{\psi'}^2 m_{\pi\pi}^2 + M_{J/\psi}^2 M_{\psi'}^2)]}{4M_{\psi'}^2}}$$

By integrating over one variable at a time, it is possible to obtain the following 1D equations for the $m_{\pi\pi}$ invariant mass spectrum and the $\cos\theta_\pi$ distribution:

$$\begin{aligned} \frac{d\sigma}{dm_{\pi\pi}} &\propto |\vec{q}|\sqrt{(q^2 - 4m_\pi^2)}\{[q^2 - \kappa(\Delta M)^2(1 + \frac{2m_\pi^2}{q^2})]^2 \\ &\quad +0.2\kappa^2[(\Delta M)^2 - q^2]^2(1 - \frac{4m_\pi^2}{q^2})^2\} \qquad (12) \\ \frac{d\sigma}{d\cos\theta} &\propto \{1.322 - 4.8597\kappa + 5.1577\kappa^2 + 1.18296\kappa(\cos^2\theta - \frac{1}{3}) \\ &\quad -2.65421\kappa^2(\cos^2\theta - \frac{1}{3}) + 0.3738\kappa^2(\cos^2\theta - \frac{1}{3})^2\} \qquad (13) \end{aligned}$$

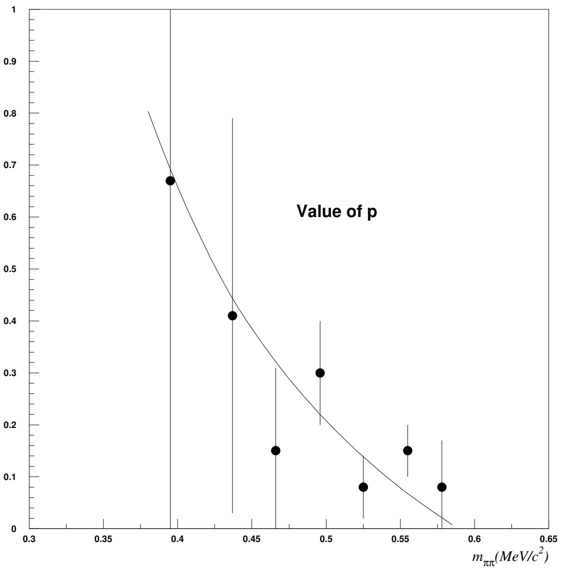

Figure 6: Plot of the interference term, p, from Eqn. 8 versus $m_{\pi\pi}$. The smooth curve is the prediction of the Novikov-Shifman model (see next section).

The $m_{\pi\pi}$ distribution is fit using Eqn. 12, as shown in Fig. 7a, and the result is given in Table 7. The fit yields $\kappa = 0.186 \pm 0.003$ with a χ^2/DOF = 1.2. We have fit the $\cos\theta$ distribution in the region $-0.8 < \cos\theta_\pi < 0.8$ using Eqn. 13. The results are shown in Fig. 7b. The fit yields $\kappa = 0.23^{+0.07}_{-0.04}$ with a χ^2/DOF = 0.7.

We have also fit the joint $\cos\theta_\pi$ and $m_{\pi\pi}$ distribution (Eqn. 11), as shown in Fig. 8. Using this approach, we obtain a $\kappa = 0.183 \pm 0.003$ and a $\chi^2/DOF = 1.2$.The results of the different fits are in good agreement. All errors are statistical only.

Mannel-Yan Model

Recently, another model, which allows D-wave like the Novikov-Shifman model, has been proposed [14]. In this model, the amplitude is

$$\begin{aligned} A &\propto \{q^2 - c_1(q^2 + |\vec{q}|^2)(1 + \frac{2m_\pi^2}{q^2}) + c_2 m_\pi^2\} \\ &\quad + \frac{3}{2}[c_1|\vec{q}|^2(1 - \frac{4m_\pi^2}{q^2})](\cos^2\theta_\pi - \frac{1}{3}), \end{aligned} \tag{14}$$

where

$$\begin{aligned} c_1 &= -\frac{g_1}{3g}(1 + \frac{g_1}{6g})^{-1} \\ c_2 &= 2(\frac{g_3}{g} - \frac{g_1}{3g} - 1)(1 + \frac{g_1}{6g})^{-1} \end{aligned} \tag{15}$$

We have fit the joint $\cos\theta_\pi$ and $m_{\pi\pi}$ distribution (Eqn. 14), as shown in Fig. 9. We obtain:

$$\frac{g_1}{g} = -0.517 \pm 0.017$$

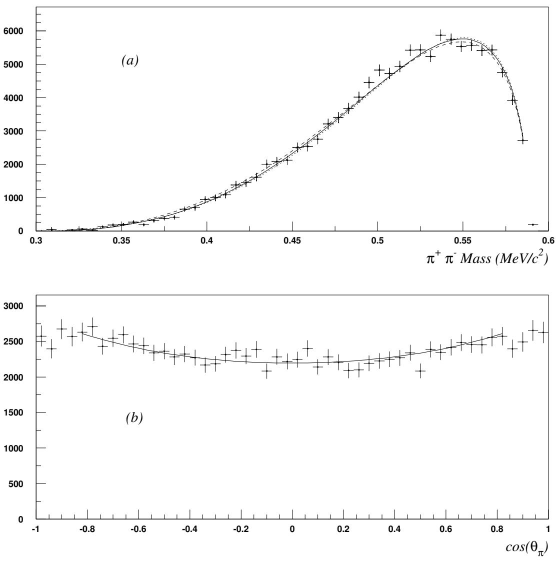

Figure 7: Fits to distributions. The results are given in Table 7. **(a)** $m_{\pi\pi}$ distribution. The points are the data corrected for efficiency, and the curves are the fit results. The smooth curve is the Novikov-Shifman model (Eqn. 12). The long-dashed curve is the Yan model without higher order corrections (Eqn. 16), and the short-dashed curve is the Voloshin-Zakarov model (Eqn. 17). **(b)** $\cos\theta_\pi$ distribution. The points are the data corrected for efficiency, and the curve is the fit result (Eqn. 13).

$$\frac{g_3}{g} \quad = \quad 0.644 \pm 0.063$$

with a $\chi^2/DOF = 1.2$.

Other Models

Other models which predict the $m_{\pi\pi}$ invariant mass spectrum are the Yan Model [5]:

$$\begin{aligned} \frac{d\sigma}{dm_{\pi\pi}} \quad &\propto \quad (PS) \times [(m_{\pi\pi}^2 - 2m_\pi^2)^2 + \frac{B}{3A}(m_{\pi\pi}^2 - 2m_\pi^2)(m_{\pi\pi}^2 - 4m_\pi^2 \\ &\qquad +2K^2(1 + \frac{2m_\pi^2}{m_{\pi\pi}^2}) + O(\frac{B^2}{A^2})], \end{aligned} \tag{16}$$

where

$$K = \frac{M_{\psi'}^2 - M_{J/\psi}^2 + m_{\pi\pi}^2}{2M_{\psi'}}$$

and the Voloshin - Zakarov Model [2]

$$\frac{d\sigma}{dm_{\pi\pi}} \propto (PS) \times [m_{\pi\pi}^2 - \lambda m_\pi^2]^2. \tag{17}$$

In the Yan model, the term $O(\frac{B^2}{A^2})$ refers to higher order (HO) terms.

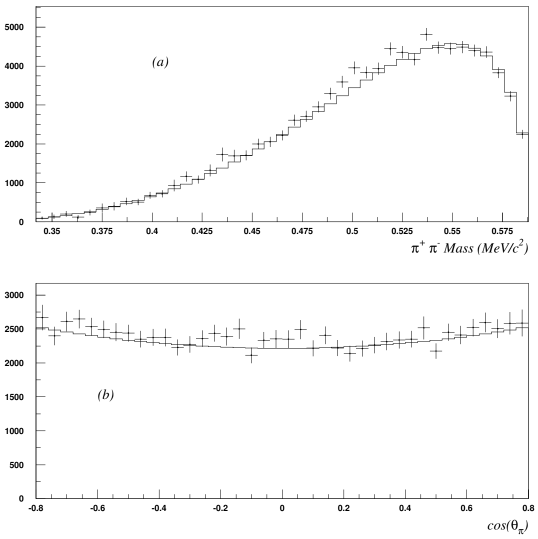

Figure 8: Fit of the 2D $\cos\theta_\pi$ versus $m_{\pi\pi}$ distribution to Eqn 11. **(a)** The 2D distribution projected in $m_{\pi\pi}$. **(b)** The 2D distribution projected in $\cos\theta_\pi$. The points are the data corrected for efficiency, and the curve is the projected fit result.

The $m_{\pi\pi}$ invariant mass spectrum has been fit with these models, as shown in Fig. 7a. As can be seen, the Novikov-Shifman and the Voloshin-Zakorov models give nearly identical fits. The Yan model, neglecting higher order terms does not agree as well with the data. Including the higher order terms [15], however, gives a fit result which is nearly identical to the other two models, as seen in Fig. 10. All the results are summarized in Table 7, along with $\psi(2S)$ and $\Upsilon(2S)$ results from Argus [16] and $\Upsilon(2S)$ results from Cleo [17]. For the $\psi(2S)$ result, Argus analyzed $\psi(2S)$ data from Mark II. Because of the running of α_s the Novikov-Shifman model is expected to yield different values for κ at the $\psi(2S)$ and the $\Upsilon(2S)$.

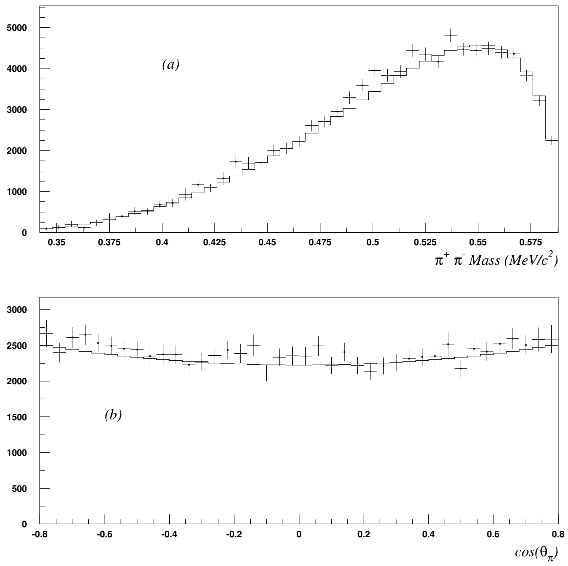

Figure 9: Fit of the 2D cos θ_π versus $m_{\pi\pi}$ distribution to Eqn 14. **(a)** The 2D distribution projected in $m_{\pi\pi}$. **(b)** The 2D distribution projected in cos θ_π. The points are the data corrected for efficiency, and the curve is the projected fit result.

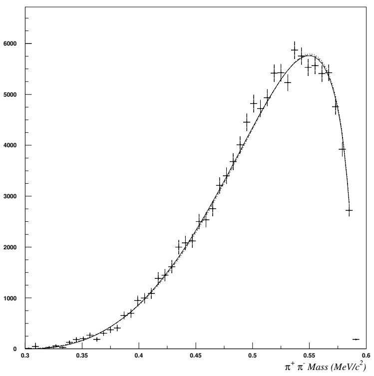

Figure 10: Fits to the $m_{\pi\pi}$ distribution. The points are the data corrected for efficiency, and the curves are the fit results. The smooth curve is the Novikov-Shifman model (Eqn. 12). The long-dashed curve is the Yan model with higher order corrections (Eqn. 16), and the short-dashed curve is the Voloshin-Zakarov model (Eqn. 17). The three models are nearly indistinguishable. The results are summarized in Table 7.

Table 7: Fit Results for the $m_{\pi\pi}$ distribution. Note that because of the running of α_s the Novikov-Shifman model is expected to yield different values for κ at the $\psi(2S)$ and the $\Upsilon(2S)$.

Model	BES $\psi(2S)$	Argus - MKII [16] $\psi(2S)$	Argus [16] $\Upsilon(2S)$	CLEO [17] $\Upsilon(2S)$
Novikov-Shifman	$\kappa = 0.186 \pm 0.003$ $\chi^2/DOF = 1.2$	0.194 ± 0.010 38/24	0.151 ± 0.009 28/19	0.146 ± 0.006
Yan	$B/A = -0.225 \pm 0.004$ $\chi^2/DOF = 1.9$	-0.21 ± 0.01	-0.154 ± 0.019 28/19	-0.145 ± 0.011
Yan (HO)	$B/A = -0.336 \pm 0.009$ $\chi^2/DOF = 1.3$			
Voloshin	$\lambda = 4.35 \pm 0.06$ $\chi^2/DOF = 1.5$		3.30 ± 0.19 27/19	3.28 ± 0.12

References

[1] G. S. Abrams *et al.* , Phys. Rev. Lett. 34, 1181 (1975).

[2] M Voloshin, V Zakharov, Phys. Rev. Lett. 45, 688(1980).

[3] V. A. Novikov and M.A. Shifman, Z. Phys.8,43(1981).

[4] M. Shifman, Phys. Rep. 209, 341 (1991).

[5] T. M. Yan, Phys. Rev. D22, 1652 (1980).

[6] Yu-Ping Kuang, T. M. Yan, Phys. Rev. D37, 1210 (1988).

[7] F. Butler *et al.* , Phys. Rev. D49, 40 (1994).

[8] F. A. Harris and Wang Meng, "Analysis Note: Number of ψ' Events", April 1998.

[9] F. A. Harris and Wang Meng, "Analysis Note: $\psi' \to \pi^+\pi^- J/\psi$, $J/\psi \to l^+l^-$ and $B(\psi' \to \pi^+\pi^- J/\psi)$", April 1998.

[10] BES Collaboration, "Determination of the J/ψ Leptonic Branching Fraction via $\psi(2S) \to \pi^+\pi^- J/\psi$", draft of Oct. 94.

[11] Robert N. Cahn, PRD 12, 3559 (1975). In the Appendix of this paper, Cahn gives the full expression for $\frac{d\Gamma}{d\Omega_\pi d\Omega_\mu d\Omega_\psi}$ in terms of all the angles involved.

[12] Belanger, et.al, PRD 39, 257 (1989).

[13] Fan Jingyun *et al.* , "An Experimental Study of $\psi' \to J/\psi\pi^+\pi^-$, April 1995.

[14] Mu-Lin Yan et al., hep-ph/9805354 (may 1998).

[15] D. Benson *et al.* , Phys. Rev. D30, 1433 (1984).

[16] H. Albrecht *et al.* , Z Phys. C 35, 283 (1987). For the $\psi(2S)$ result, Mark II data was used.

[17] CLNS 98/1504, CLEO CLEO 98-1, J. Alexander et al., Submitted to Phys. Rev. D